The Sodium-Coupled Neutral Amino Acid Transporter SNAT2 Mediates an Anion Leak Conductance that Is Differentially Inhibited by Transported Substrates

Zhou Zhang and Christof Grewer
University of Miami School of Medicine, Miami, Florida 33136

ABSTRACT The sodium-coupled neutral amino acid transporter SNAT2 mediates cellular uptake of glutamine and other small, neutral amino acids. Here, we report the existence of a leak anion pathway associated with SNAT2. The leak anion conductance was increased by, but did not require the presence of, extracellular sodium. The transported substrates L-alanine, L-glutamine, and α-(methylamino)isobutyrate inhibited the anion leak conductance, each with different potency. A transporter with the mutation H-304A did not catalyze alanine transport but still catalyzed anion leak current, demonstrating that substrate transport is not required for anion current inhibition. Both the substrate and Na^+ were able to bind to the $SNAT2_{H\text{-}304A}$ transporter normally. The selectivity sequence of the $SNAT2_{H\text{-}304A}$ anion conductance was $SCN^- \gg NO_3^- > I^- > Br^- > Cl^- > Mes^-$. Anion flux mediated by the more hydrophobic anion SCN^- was not saturable, whereas nitrate flux demonstrated saturation kinetics with an apparent K_m of 29 mM. SNAT2, which belongs to the SLC38 family of transporters, has to be added to the growing number of secondary, Na^+-coupled transporters catalyzing substrate-gated or leak anion conductances. Therefore, we can speculate that such anion-conducting pathways are general features of Na^+-transporting systems.

INTRODUCTION

System A is a ubiquitous Na^+-dependent amino acid transporter that actively transports small, zwitterionic, neutral amino acids with short, unbranched side chains, such as alanine, serine, and glutamine, across cell membranes (1–4). It has the unique ability to transport *N*-methylated amino acids such as α-(methylamino)isobutyric acid (MeAIB) (5–7) and is upregulated by amino acid starvation (8) and hormones (9). Recent data show that system A is encoded by three different members of the SLC38 gene family (Slc38a1, Slc38a2, and Slc38a4), giving rise to the three subtypes of this sodium-coupled neutral amino acid transporter (SNAT): SNAT1, SNAT2, and SNAT4 (also referred to as ATA1, ATA2, and ATA3, respectively) (4,7,10–14). Inward amino acid transport by these systems is electrogenic and coupled to inward charge movement. Functionally, SNAT1 and SNAT2 are thought to operate via similar mechanisms (4,11).

As in other electrogenic secondary transport systems, application of transported substrates to SNAT1 or SNAT2 elicits coupled transport currents in *Xenopus* oocytes expressing the transporters (11,13,15,16). In addition to these coupled current components, some transporters also show currents that are not stoichiometrically coupled to substrate transport. Many transporters catalyze Na^+ leak currents, as found for example in the Na^+-coupled glucose transporters and the phosphate transporters (17–19). A Na^+ leak current has also been reported for SNAT1 (13). Other transporters catalyze anion currents. The excitatory amino acid transporters (EAATs), for example, are associated with a glutamate-gated anion conductance (20–26). In some glutamate transporter subtypes, such as EAAT5, this anion conductance is so prominent that it masks the electrical activity generated by coupled glutamate transport (27). An uncoupled anion conductance, which is gated by the transported substrate, has also recently been reported for the dopamine transporter (28). It is unknown whether system A transporters also exhibit such uncoupled anion conductances.

Here, we report the characterization of an anion leak conductance of rat SNAT2, the second member of the system A family of neutral amino acid transporters, expressed in human embryonic kidney cells (HEK293T). This anion leak pathway is differentially inhibited by the application of transported substrates to SNAT2, such as alanine, glutamine, and MeAIB, with MeAIB showing the strongest inhibitory effect. The amplitude of this anion conductance is magnified in a transporter with the mutation His-304 to alanine in the sixth predicted transmembrane domain of the SNAT2 transporter molecule (Fig. 1). In contrast to the anion conductance, alanine transport is strongly inhibited by this mutation. However, both Na^+ and substrate binding are only weakly affected by the mutation. The permeability of the anion leak conductance is higher for SCN^- than for Cl^-, indicating a preference for hydrophobic anions. Binding of Na^+ to SNAT2 is not required to activate this leak anion conductance, but it increases its magnitude. Our data, for the first time to our knowledge, show the existence of an anion leak conductance for transporters of the SLC38 family and add to the mounting evidence that

Submitted November 9, 2006, and accepted for publication December 27, 2006.

Address reprint requests to Christof Grewer, PhD, Dept. of Physiology and Biophysics, University of Miami School of Medicine, 1600 NW 10th Avenue, Miami, FL 33136. Tel.: 305-243-1021; Fax: 305-243-5931; E-mail: cgrewer@med.miami.edu.

© 2007 by the Biophysical Society

0006-3495/07/04/2621/12 $2.00

doi: 10.1529/biophysj.106.100776

```
SNAT1 RAT     279 TVYALPTIAFAFVCHPSVLPI 299
SNAT1 HUMAN   275 TVYALPTIAFAFVCHPSVLPI 295
SNAT2 RAT     290 TVYAVPILTFSFVCHPAVLPI 310
SNAT2 HUMAN   292 TVYAVPILIFSFVCHPAVLPI 312
SNAT4 RAT     332 TAYAIPILAFAFVCHPEVLPI 352
SNAT4 HUMAN   332 TAYAIPILVFAFVCHPEVLPI 352
SNAT3 RAT     286 TAYTIPIMAFAFVCHPEVLPI 306
SNAT3 HUMAN   286 TAYTIPIMAFAFVCHPEVLPI 306
SNAT5 RAT     257 MSYTVPIMAFAFVCHPEVLPI 277
SNAT5 HUMAN   258 MSYTVPIMAFAFVCHPEVLPI 278
```

FIGURE 1 Sequence alignment of the putative sixth transmembrane domain of the SLC38 (SNAT) family. The highly conserved SNAT2 His-304 residue mutated to alanine is highlighted.

anion-conducting behavior is a general property of Na^+-coupled secondary transport systems.

MATERIALS AND METHODS

Molecular biology and transient expression

The cDNA coding for the rat SNAT2, which was kindly provided by H. Varoqui, was subcloned into the SacI and NheI sites of a modified pBK-CMV vector (Δ[1098-1300]) (Stratagene, La Jolla, CA), containing the CMV promoter for mammalian expression. Wild-type SNAT2 was used for site-directed mutagenesis according to the QuikChange protocol (Stratagene), as described by the supplier. The primers for mutation experiments were obtained from the DNA core lab, Department of Biochemistry at the University of Miami School of Medicine. The complete coding sequences of mutated SNAT2 clones were subsequently sequenced. Wild-type and mutant transporter constructs were used for transient transfection of subconfluent human embryonic kidney cell (HEK293T/17, ATCC number CRL 11268) cultures using FuGENE 6 Transfection Reagent (Roche, Indianapolis, IN) according to the instructions of the supplier. The 293T/17 cell line is a derivative of the 293T cell line into which the gene for SV40 T-antigen was inserted. Electrophysiological recordings were performed between days 1 and 3 postransfection.

Electrophysiology

SNAT2-mediated currents were recorded with an Adams & List EPC7 amplifier (Heka Elektronik, Lambrecht, Germany) under voltage-clamp conditions in the whole-cell current-recording configuration. The typical resistance of the recording electrode was 2–3 MΩ; the series resistance was 5–8 MΩ. Because the currents induced by substrate, anion, or cation application were small (typically <500 pA), series resistance (R_S) compensation had a negligible effect on the magnitude of the observed currents (<4% error). Therefore, R_S was not compensated. The extracellular bath buffer solution contained (mM): 140 sodium methanesulfonate (NaMes), 2 magnesium gluconate ($MgGlu_2$), 2 calcium gluconate ($CaGlu_2$), 30 Tris, pH 8.0. All experiments were conducted at an extracellular pH of 8.0 because amino acid transport by SNAT2 is pH dependent and the transport rate is maximal at pH 8.0. For the determination of anion selectivity, the Mes^- anion was substituted with different anions. For testing the $[Na^+]$ dependence of the currents, Na^+ in the extracellular solution was replaced with NMG^+ (*N*-methylglucamine). The pipette solution contained (in mM): 140 KMes or KSCN, 2 $MgGlu_2$, 10 EGTA, HEPES, pH 7.3. For determining the voltage dependence of SNAT2 alanine transport, a combined voltage ramp/solution exchange protocol was used. In this protocol, the cell membrane was initially held at 0 mV, before ramping the voltage to its final value (−90 to +60 mV) within 2 s. Two seconds after establishing the new voltage, the extracellular solution was changed from no alanine to the final concentration of alanine, followed by ramping the voltage back to 0 mV.

The currents were low-pass filtered at 1–10 kHz (Krohn-Hite 3200) and digitized with a digitizer board (Axon Instruments (Foster City, CA) Digidata 1200) at a sampling rate of 10–50 kHz, which was controlled by software (Axon PClamp). All the experiments were performed at room temperature.

Rapid solution exchange

Rapid solution exchange was performed as described previously (15). Briefly, substrates were applied to a voltage-clamped, SNAT2-expressing cell suspended at the tip of the current recording electrode by means of a quartz tube (opening diameter: 350 μm) positioned at a distance of ~0.5 mm to the cell. The linear flow rate of the solutions emerging from the opening of the tube was ~5–10 cm/s, resulting in typical rise times of the whole-cell current of 30–50 ms (10%–90%).

Data analysis

Nonlinear regression fits of experimental data were performed with Origin (Microcal Software, Northampton, MA) or Clampfit (pClamp8 software, Axon Instruments). Dose response relationships of currents were fitted with a Michaelis-Menten-like equation, yielding K_m and I_{max}. Endogenous electrogenic alanine transport activity in HEK293T cells, as measured by current recording from nontransfected cells, is minimal (see Results section). For the Na^+ concentration dependence of the leak current, the dose-response data were corrected by subtraction of the nonspecific component of the current, which increases linearly with increasing $[Na^+]$. The nonspecific component was determined from nontransfected HEK293 cells. Each experiment was repeated at least three times with at least two different cells. The error bars represent mean ± SD, unless stated otherwise. Maximum SNAT2-dependent currents, I_{max}, vary approximately by a factor of 3 between different cells, depending on the expression levels of each individual cell. Such changes in expression levels did not affect the K_m for the amino acid. The I_{max} values were obtained by averaging the I_{max} values from these individual cells.

Theoretical current voltage relationships for leak anion currents (see Fig. 3, *E* and *F*) were calculated using the Goldman-Hodgkin-Katz current equation (29):

$$I_{leak} \approx \frac{P_{anion} F V' ([anion]_{out} - [anion]_{in} \exp(-V'))}{1 - \exp(-V')}, \quad (1)$$

where $V' = FV/RT$, F is the Faraday constant, T the temperature, R the gas constant, V the transmembrane potential, and P_{anion} the permeability of a single SNAT2 molecule for anions. The current voltage relationship of the alanine-induced transport current (see Fig. 3 *F*) was empirically approximated by a sum of a current component that exponentially depends on the voltage and a voltage-independent component. Anion permeabilities relative to SCN^- were calculated using the Goldman-Hodgkin-Katz voltage equation.

RESULTS

Functional characterization of SNAT2 expressed in HEK293 cells

Application of L-alanine (10 mM) to voltage-clamped, SNAT2-expressing HEK293T cells resulted in inwardly directed whole-cell currents in the presence of Na^+ at the extracellular side of the membrane (Fig. 2 *A*, at 0 mV transmembrane potential). The current evoked by SNAT2 was on average −120 ± 40 pA (Fig. 2 *B*, $n = 7$). This current was specifically carried by SNAT2, since it was abolished in the absence of Na^+, as reported previously for this transport system. Furthermore, nontransfected HEK293 control cells

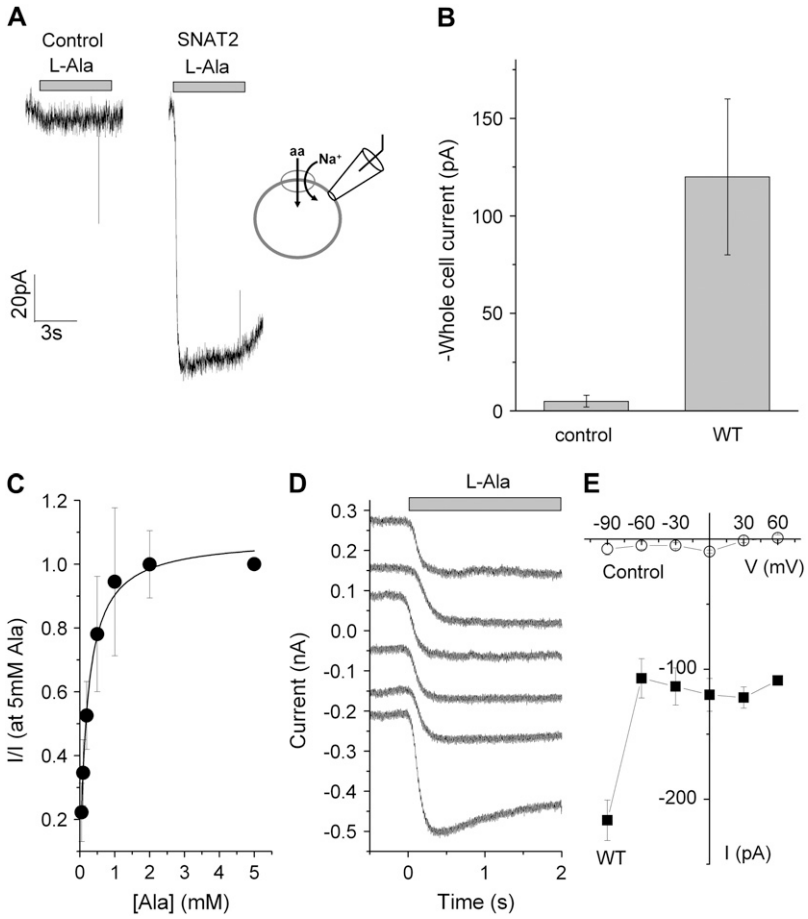

FIGURE 2 Functional characterization of SNAT2 expressed in HEK293 cells. (*A*) Currents induced by application of 10 mM alanine to control cells (*left panel*) and SNAT2-expressing cells (*right panel*). The bath solution contained 140 mM NaMes, and the pipette solution contained 140 mM KMes at 0 mV transmembrane potential. (*B*) Statistical analysis of transport currents between $SNAT2_{WT}$-expressing and nontransfected cells (control). Leak currents were subtracted. The large error bar of the currents in the SNAT2-expressing cells is caused by the up to threefold differences in expression levels between different cells. (*C*) The apparent affinity for the substrate L-alanine of $SNAT2_{WT}$ was determined by recording substrate-induced transport current as a function of [alanine] at 0 mV. (*D*) Voltage dependence of representative L-alanine-induced transport currents. Saturating concentrations of L-alanine (10 mM) were applied in 140 mM NaMes at the time indicated by the bar. (*E*) Average alanine-induced current-voltage relationships in nontransfected cells (control, *open circles*) and $SNAT2_{WT}$-expressing cells (*solid squares*).

showed only a little response to 10 mM alanine (-7 ± 4 pA, Fig. 2, *A* and *B*, $n = 8$). The L-alanine-induced currents were dependent on the extracellular alanine concentration (Fig. 2 *C*). This concentration dependence followed Michaelis-Menten kinetics with a K_m of 200 ± 18 μM ($n = 5$). This K_m value is in agreement with previously published values of 200 μM (4) and 230 μM (2) for SNAT2 expressed in *Xenopus* oocytes. Next, we determined the voltage dependence of SNAT2 transport currents. We used a combined voltage ramp/solution exchange protocol for this purpose (see Materials and Methods). SNAT2 L-alanine-evoked transport currents (at a saturating concentration of amino acid) showed a relatively small dependence on the membrane potential (V_m) from -60 mV to $+60$ mV (Fig. 2, *D* and *E*, *solid squares*) but a steep increase at a potential of -90 mV. Control cells showed only a little response to alanine within the range of membrane potentials tested (Fig. 2 *E*, *open circles*). Alanine-evoked transport currents did not reverse within the voltage range tested, as expected for the zero-*trans* conditions applied in these experiments (no Na^+ and alanine were present on the intracellular side of the membrane). Although this current-voltage relationship is consistent with the proposed stoichiometry of alanine and Na^+ cotransport of 1:1, other coupling stoichiometries are not excluded by these data. Finally, SNAT2-transfected HEK293 cells responded to the application of MeAIB (*N*-methyl-α-isubutyric acid, 10 mM), a selective system A substrate, with inward currents (-62 ± 20 pA, $n = 7$) (see Fig. 4), whereas nontransfected control cells showed no significant response to MeAIB (data not shown). Together, these data demonstrate that SNAT2 expressed in HEK293 cells has properties very similar to the transporter expressed in *Xenopus* oocytes.

SNAT2 catalyzes an uncoupled leak anion conductance that is differentially inhibited by transported substrates

In the previous experiments we used Methanesulfonate (Mes^-) as the main anion. When intracellular Mes^- was replaced with SCN^-, a hydrophobic anion that is known to carry large uncoupled anion currents in glutamate transporters (20), SNAT2-expressing cells showed a large background current in the absence of alanine (Fig. 3 *A* at $t < 0$ s and Fig. 3 *B*, *open squares*), which was inwardly directed at potentials more negative than $+25$ mV. At negative membrane potentials alanine application resulted in the partial suppression of this background current, as shown in Fig. 3 *A* at $t > 0$ s and Fig. 3 *B* (*solid squares*). At -90 mV the current was on average 360 ± 130 pA ($n = 5$) larger in the absence of alanine than in its presence. These data suggest that at negative

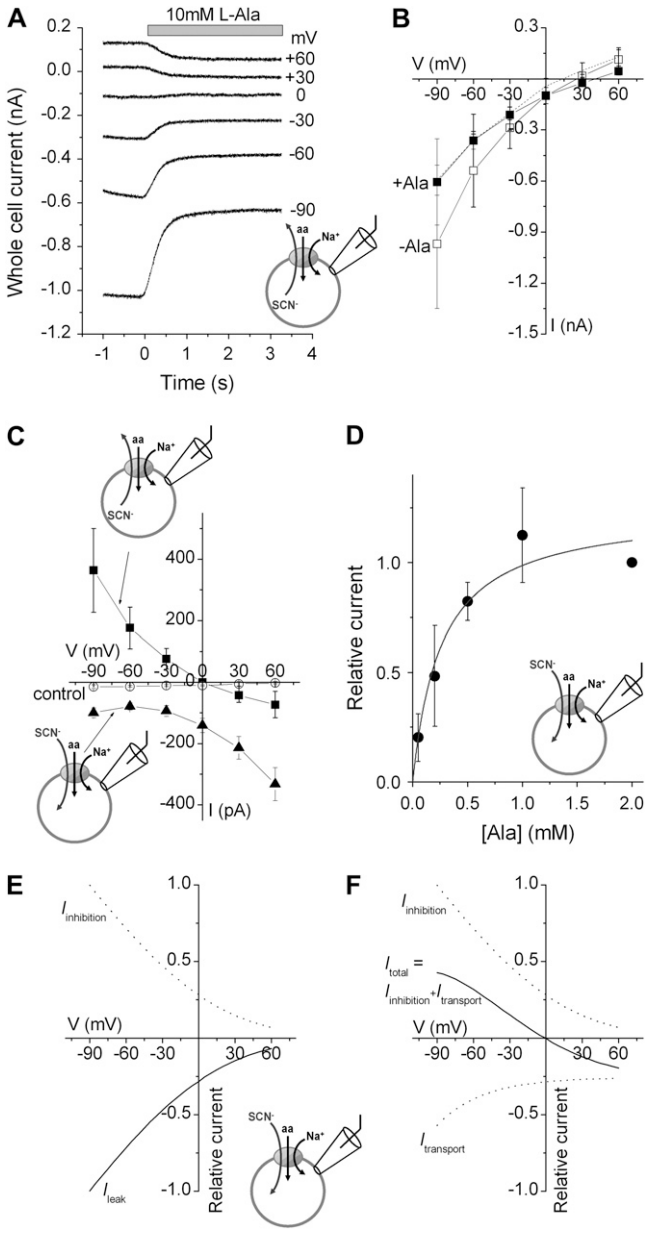

FIGURE 3 SNAT2 catalyzes an uncoupled leak anion conductance that is inhibited by alanine. (*A*) Voltage dependence of alanine-sensitive $SNAT2_{WT}$ currents in the presence of 140 mM intracellular KSCN and 140 mM extracellular NaMes. A saturating concentration of L-alanine (10 mM) was applied at $t = 0$ s, as indicated by the bar. (*B*) Current-voltage relationships in $SNAT2_{WT}$-expressing cells in the absence (*open squares*) and in the presence (*solid squares*) of 10 mM L-alanine in the presence of 140 mM intracellular SCN^-. The dashed lines show currents in nontransfected control cells recorded under the same conditions (both *dashed lines* are superimposable). (*C*) Current-voltage relationships of L-alanine-sensitive currents (10 mM alanine) in $SNAT2_{WT}$ obtained after subtraction of the current in the absence from that in the presence of alanine with 140 mM SCN^- present only in the pipette (*solid squares*), and 140 mM SCN^- only present on the extracellular side (*solid triangles*). The open circles show data from control cells not expressing SNAT2 in the presence of intracellular SCN^-. (*D*) The apparent affinity for L-alanine of $SNAT2_{WT}$ was determined by recording the alanine-sensitive current as a function of [alanine] at 0 mV in the presence of 140 mM extracellular SCN^-. (*E*) Simulation of the leak anion current (I_{leak}) and the alanine-inhibition of the leak anion current ($I_{inhibition}$) obtained from Eq. 1. (*F*) Simulation of total (I_{total}) L-alanine-sensitive currents. The total current in the presence of intracellular SCN^- (I_{total}) was calculated as the sum of the alanine-inhibited leak anion current component ($I_{ihibition} = -I_{leak}$) and the alanine-induced transport current component ($I_{transport}$).

membrane potentials alanine inhibits a tonic inward current, which is probably caused by SCN^- outflow. Alanine-sensitive currents were not caused by K^+ leaving the cell since the currents were unchanged after substitution of intracellular K^+ with NMG^+ (data not shown). The data in Fig. 3 *B* also show that background current is also present in nontransfected control cells (*dashed lines*). However, no alanine sensitivity of the background current was observed in these control cells. This background current may be due to alanine-insensitive, unspecific anion and cation conductances in the HEK293T cells. To eliminate unspecific currents from our analysis, the data presented throughout the remainder of this work will only show the SNAT2-specific, amino acid-sensitive components of these currents, which were obtained by subtracting the current in the absence of alanine from that in its presence. A current voltage relationship of this subtracted, alanine-sensitive current in the presence of 140 mM intracellular SCN^- is shown in Fig. 3 *C* (*solid squares*).

The alanine-sensitive current was outwardly directed at negative potentials and inwardly directed at positive potentials, showing a reversal potential of -1 ± 4 mV. This reversal potential was independent of the expression level of the cell (Supplementary Materials Fig. 1). We hypothesize that the outward current at negative voltages is caused by alanine inhibition of a tonic anion leak current. To test this hypothesis, we reverted the anion concentration gradient across the membrane, applying SCN^- only to the extracellular side. The data in Fig. 3 *C* (*solid triangles*) show that alanine-sensitive, SNAT2-specific currents were always inwardly directed under these conditions. Control cells did not respond to alanine application in the presence of intracellular SCN^- within the voltage range tested (Fig. 3 *C*, *open circles*), excluding the possibility that the anion conductance is caused by an alanine-sensitive anion channel or transporter natively expressed in HEK293T cells. The apparent K_m value of anion current inhibition by alanine was 260 ± 100 μM in the presence of extracellular SCN^- (at 0 mV, Fig. 3 *D*, compared to 200 μM in the presence of Mes^-), suggesting that the inhibition of the anion conductance by alanine is triggered by the same substrate-binding process as the activation of the transport current. To summarize the data described in this section, we propose that the total alanine-sensitive current in the presence of permeating anions (I_{total}) is the sum of the alanine-inhibited leak anion current component ($I_{inhibition} = -I_{leak}$, Fig. 3 *E*) and the alanine-induced transport current component ($I_{transport}$), as illustrated by the theoretically calculated currents (using Eq. 1) in Fig. 3 *F* for SCN^- present only on the intracellular side. Further experiments to test this proposal are shown in the next sections.

MeAIB sensitivity is thought to be the hallmark of system A transporters (7). Consistently, we found MeAIB to be a transported substrate of SNAT2 (Fig. 4 *A*, *top panel*). However, it is transported at a lower steady-state rate than alanine. Thus, it induces smaller SNAT2 transport current (-63 ± 20 pA, $n = 5$). If the total current in the presence of intracellular SCN^- is a sum of the transport current and the inhibited leak anion current, as proposed in the last section, the reversal potential should be shifted to more positive values because the MeAIB transport component should contribute less to the total current. Consistent with this expectation, the reversal potential for the MeAIB-sensitive current was $+20 \pm 7$ mV (Fig. 4 *B open circles* and Fig. 4 *C*). Glutamine is an important substrate of SNAT2, which is known to be transported at a lower steady-state rate than alanine (4). Therefore, in analogy to MeAIB, glutamine-sensitive currents should also show a right-shifted reversal potential as compared to alanine-sensitive currents in the presence of intracellular SCN^-. However, the opposite was the case with glutamine-sensitive currents showing a reversal potential of -22 ± 7 mV (Fig. 4 *B solid squares*). These results, which are summarized in Fig. 4 *C*, indicate that the transport component contributes to a larger extent to the total current for glutamine than for MeAIB and alanine. Together, these results suggest that substrates vary in their ability to inhibit the SNAT2 leak anion conductance.

To further test the hypothesis that SNAT2 catalyzes a leak anion conductance, we measured current-voltage relationships of alanine-sensitive currents (10 mM) in the presence of different concentrations of intracellular SCN^-. As shown in Fig. 5 *A*, the current-voltage relationships changed with decreasing $[SCN^-]_{int}$, accompanied by a shift of the reversal potential to more negative potentials. This shift in reversal potential was due to the increasing contribution of the transport component to the total current at lower internal $[SCN^-]$. At an intracellular SCN^- concentration of 20 mM the alanine-sensitive current was always inwardly directed, indicating that the alanine-induced inhibition of the anion leak current was unable to overcome the inwardly directed transport component of the current, even at a transmembrane potential of -90 mV. Therefore, we could not determine a reversal potential under these ionic conditions. Fig. 5 *B* shows the dependence of the reversal potential on $[SCN^-]_{int}$. Although the slope of 87 ± 16 mV is slightly steeper than the 58 mV change per decade of change in $[SCN^-]$ in reversal potential expected for a pure anion conductance, this analysis is consistent with the total alanine-sensitive current being independently caused by two components: the alanine-induced transport component and the alanine-inhibited leak anion component.

One explanation for the steeper than expected slope could be that the anion changes the transport rate for the substrate such that increasing intracellular $[SCN^-]$ reduces the transport component of the current. This hypothesis would be consistent with a previous report showing that MeAIB transport by SNAT2 is inhibited in the absence of chloride (30). These results indicated that the anion has a direct effect on the amino acid transport rate. To test this hypothesis, we determined the dependence of the reversal potential of the alanine-sensitive current on extracellular $[SCN^-]_{out}$ in a mutant transporter ($SNAT2_{H\text{-}304A}$) that does not catalyze transport current at negative membrane potentials (see next section). These experiments were performed in the presence of low intracellular $[SCN^-]$ (10 mM). The reversal potential was shifted by -47 mV when the extracellular $[SCN^-]$ was increased 10-fold (Supplementary Materials Fig. 2), suggesting that the steeper than expected slope of the reversal potential-log$[SCN^-]$ relationship of the wild-type transporter is caused by a modulation of the transport current component by the permeating anion.

Inhibition of the leak anion conductance by alanine does not require amino acid transport

One possible explanation for the above data would be that alanine inhibits the leak anion conductance of SNAT2 by being transported across the membrane. Thus, the transporter would spend more time in states associated with substrate translocation than in the anion-conducting state(s). To test this idea, we measured anion currents in the H-304A mutant transporter, which is defective in steady-state substrate transport (Fig. 6 *A*). This mutation was initially generated to test for possible proton-acceptor sites on SNAT2 that are

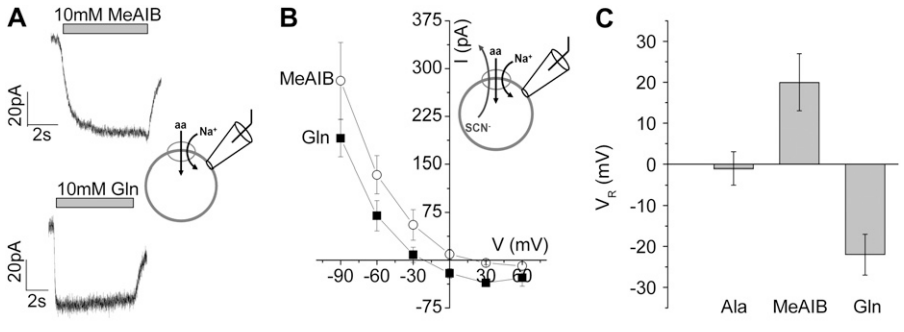

FIGURE 4 The extent of inhibition of the leak anion conductance depends on the transported substrate. (*A*) Transport currents activated at 0 mV by application of L-glutamine (*bottom panel*) and MeAIB (*top panel*) to SNAT2 at concentrations indicated by the bar (Mes^- was used as the anion on both sides of the membrane). (*B*) Average current-voltage relationships of substrate-sensitive currents induced by 10 mM glutamine (*solid squares*) and 10 mM MeAIB (*open circles*) to SNAT2 in the presence of 140 mM intracellular SCN^- ($n = 4$). The main anion in the bath buffer was Mes^-. (*C*) Statistical analysis of reversal potentials for substrate-induced currents for alanine, glutamine, and MeAIB. The ionic conditions were as in (*B*).

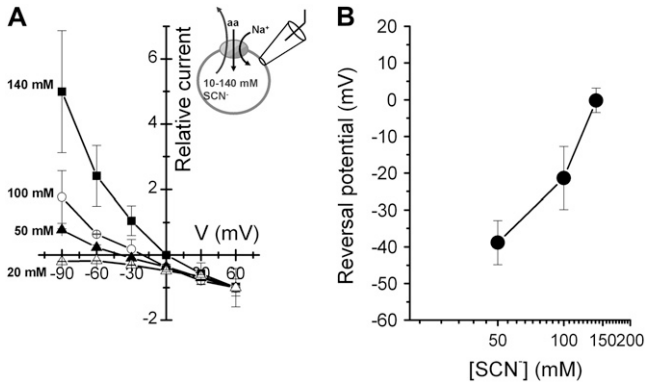

FIGURE 5 Intracellular [SCN^-] determines the reversal potential of the alanine-sensitive current. (*A*) Mean current amplitudes for various internal [SCN^-] in the presence of 10 mM external L-alanine. SCN^- was substituted equimolarly with Mes^-. The currents were normalized to the currents recorded at +60 mV. (*B*) Reversal potential-[SCN^-] relationship of $SNAT2_{WT}$ anion currents.

involved in H^+-modulation of amino acid transport but was then used in this work because of its lack of steady-state alanine transport. Application of 10 mM alanine to SNAT2 with the mutation H-304A did not induce significant transport currents at 0 mV (Fig. 6 *A*). Although a small transport activity was observed at positive transmembrane potentials (Fig. 6 *A*), the transporter was fully inactive at negative potentials up to −90 mV. The presence of transport current at positive potentials may indicate the existence of a transport reaction of opposite voltage dependence in $SNAT2_{H\text{-}304A}$ that is hidden in the wild-type transporter, or a leak Na^+ current. This phenomenon, although interesting, may be addressed in a future study. As in $SNAT2_{WT}$, 10 mM alanine application in the presence of intracellular SCN^- resulted in an inhibition of a tonic inward current (Fig. 6, *B* and *C*), inducing apparent outward current (Fig. 6 *B*, 104 ± 59 pA, $n = 5$, 0 mV). In contrast to $SNAT2_{WT}$ (Fig. 3 *C*), the alanine-sensitive current did not reverse within the potential range studied (−90 to +60 mV, Fig. 6 *D*, *solid squares*). As expected for a current carried purely by SCN^-, the direction of the current was reversed when SCN^- was only present in the extracellular buffer (Fig. 6 *D*, *solid triangles*). The presence of alanine-sensitive current in $SNAT2_{H\text{-}304A}$ indicates that this mutation did not interfere with alanine binding. The K_m determined for alanine inhibition of the leak anion current was 29 ± 5 μM ($n = 5$, data not shown). As in wild-type SNAT2, these currents were caused by inhibition of the leak anion conductance, as shown by recording I-V relationships with SCN^- present only on the intracellular or only on the extracellular side of the membrane (Fig. 6 *D*). However, in contrast to $SNAT2_{WT}$ the inhibition of these anion currents was not contaminated by the presence of the transport current component (in the negative voltage range). Thus, the H-304A-mutant transporter allowed us to study the anion current component in isolation. Together, these data suggest that amino acid binding, but not transport, is required for the inhibition of the leak anion current.

The presence of extracellular Na^+ increases the leak anion conductance

Glutamate transporters also exhibit a leak anion conductance, which is activated by extracellular Na^+ (31). Therefore, we tested whether such a requirement for Na^+ is also found for the SNAT2 anion conductance. Large inward currents were observed in HEK293T cells expressing $SNAT2_{WT}$ (Fig. 7 *B*, −59 ± 33 pA, $n = 5$, 0 mV) or $SNAT2_{H\text{-}304A}$ (Fig. 7 *B*, −340 ± 120 pA, $n = 6$, 0 mV) upon switching from Na^+-free extracellular solution (NMG^+ replacement) to 140 mM Na^+ in the absence of amino acid

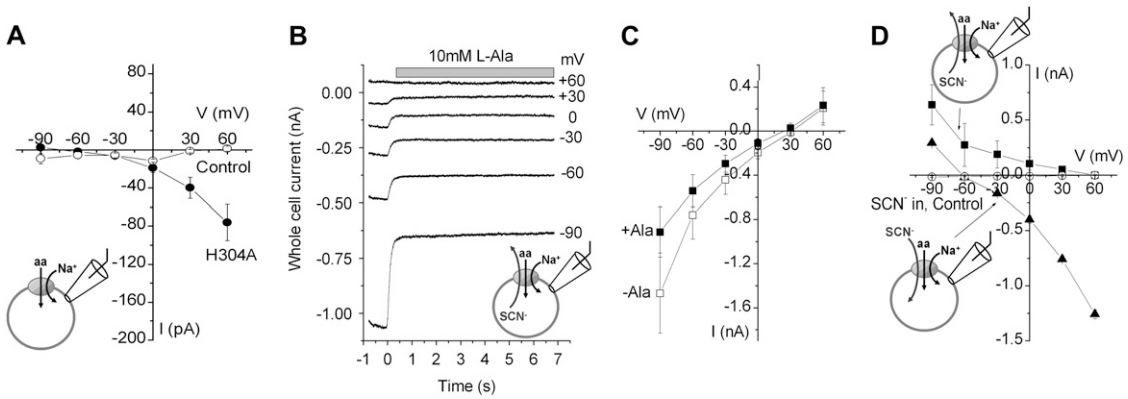

FIGURE 6 $SNAT2_{H\text{-}304A}$ mediates the leak anion conductance but little alanine transport activity. (*A*) Comparison of alanine-induced transport currents between $SNAT2_{H\text{-}304A}$-expressing and nontransfected cells (control). The bath solution contained NaMes, and the pipette solution contained KMes. Leak currents were subtracted. (*B*) Voltage dependence of $SNAT2_{H\text{-}304A}$ alanine-sensitive currents in the presence of 140 mM intracellular KSCN and 140 mM extracellular NaMes. Saturating concentrations of L-alanine (10 mM) were applied at $t = 0$ s, as indicated by the bar. (*C*) Current-voltage relationships of $SNAT2_{H\text{-}304A}$ currents in the absence (*open squares*) and in the presence (*solid squares*) of 10 mM L-alanine with intracellular 140 mM SCN^-. (*D*) Current-voltage relationship of L-alanine-sensitive currents in $SNAT2_{H\text{-}304A}$ (10 mM alanine) with SCN^- present only in the pipette (*solid squares*), SCN^- only present on the extracellular side (*solid triangles*). The open circles show data from control cells not expressing $SNAT_{H\text{-}304A}$ in the presence of intracellular SCN^-.

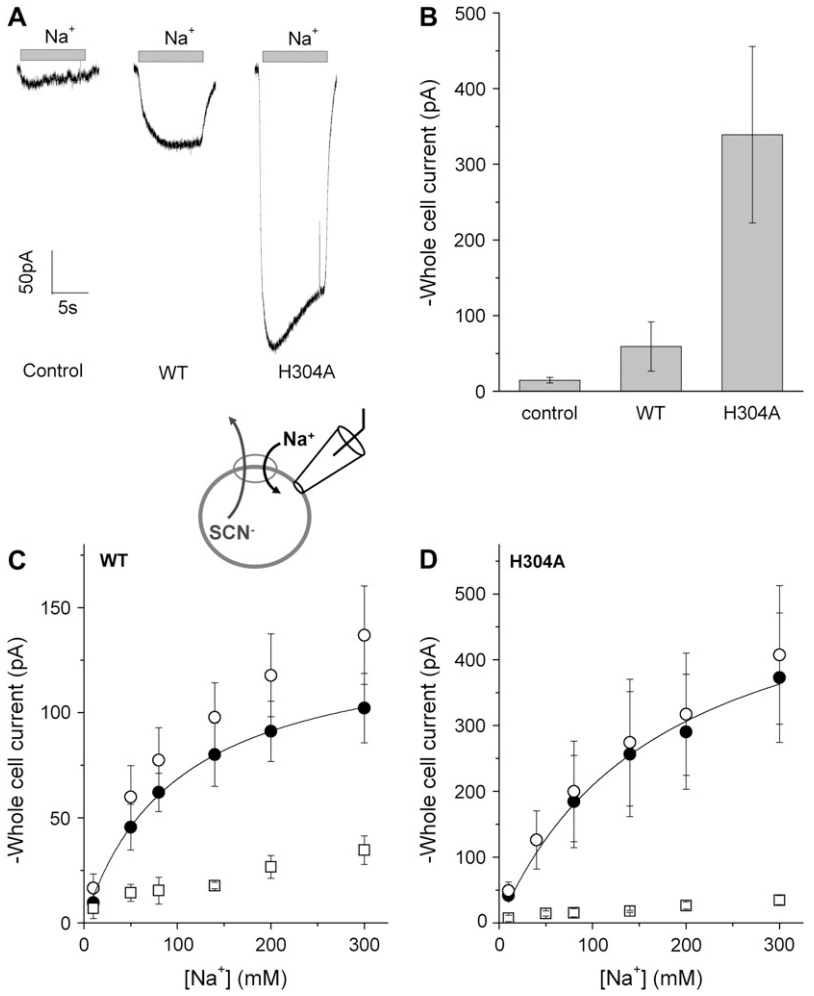

FIGURE 7 Leak anion currents are activated by extracellular Na^+. Whole-cell current recordings were performed with a KSCN-based pipette solution (140 mM) and at 0 mV transmembrane potential. (*A*) Comparison of typical leak anion currents induced by the application of 140 mM extracellular Na^+ between nontransfected cells (control), $SNAT2_{WT}$, and $SNAT2_{H\text{-}304A}$-expressing cells, as indicated by the gray bars. (*B*) Statistical analysis of average Na^+-induced currents as the ones shown in (*A*). (*C*) and (*D*) show leak anion currents as a function of extracellular $[Na^+]$ for $SNAT_{WT}$ (*C*) and $SNAT2_{H\text{-}304A}$ (*D*), respectively (*solid circles*, after subtracting the unspecific currents, *open squares*, determined from nontransfected cells). The solid lines represent fits to the Hill equation with a Hill coefficient of $n = 1$. The open circles in *C* and *D* are results from the original experiments before subtraction of the unspecific leak currents (*open squares*) determined in nontransfected control cells.

(original traces are shown in Fig. 7 *A*). Although nontransfected control cells showed small current responses to $[Na^+]$ jumps at the same conditions (Fig. 7, *A* and *B*), current evoked by $SNAT2_{WT}$ was fourfold that observed for control cells, whereas current was 23-fold over control for $SNAT2_{H\text{-}304A}$. The leak current was Na^+ concentration dependent but did not saturate at physiological $[Na^+]$ (Fig. 7, *C* and *D*). Kinetic analysis indicated that the affinity of the transporters for Na^+ was only slightly decreased for $SNAT2_{H\text{-}304A}$ ($K_m = 175 \pm 37$ mM, $n = 5$) compared to $SNAT2_{WT}$ ($K_m = 100 \pm 7$ mM, $n = 5$) at pH 8.0. This result indicates that Na^+ binding is not strongly affected by the mutation. Although the Na^+-free transporter also conducts anions (see next section), our results show that the full activation of the leak anion conductance requires the presence of Na^+ in the extracellular solution.

Anion leak currents are present in the absence of extracellular Na^+

With SCN^- in the recording pipette solution and Cl^- in the bath solution, the current-voltage relationship was determined with a double solution exchange protocol, first from NMGCl to NaCl, and second from NaCl to NaCl plus 10 mM L-alanine (Fig. 8 *A*, the intracellular solution contained 140 mM SCN^-), to determine whether the anion leak was already present in the absence of extracellular Na^+. The results of this experiment are shown in Fig. 8, *A* and *B*. The inward current caused by SCN^- outflow was larger in the absence of Na^+ than in the presence of both Na^+ and alanine. The specific, SNAT2-carried current was obtained by subtracting the NaCl/alanine-sensitive current (indicated by the *arrow* at time point B in Fig. 8 *A*) from that in the presence of NMGCl only (indicated by the *arrow* at time point A in Fig. 8 *B*, $n = 3$). From these data it is clear that alanine in the presence of Na^+ inhibits an anion leak current that is already present in the absence of extracellular Na^+.

Ion selectivity of the transporter-associated anion conductance

The ion selectivity of the SNAT2 anion conductance was determined by changing the extracellular anion while keeping

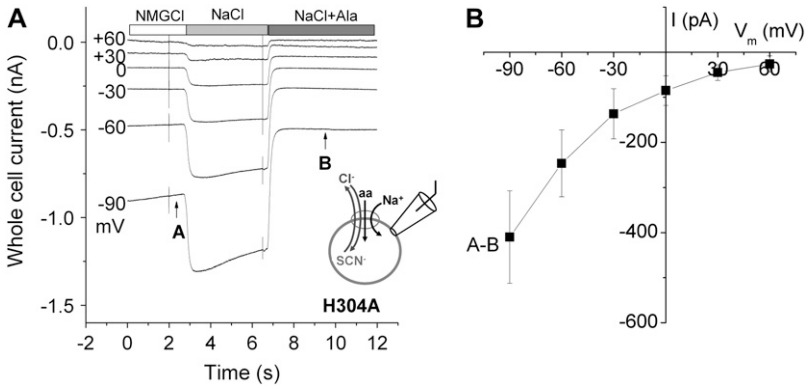

FIGURE 8 Leak anion currents are present in the absence of extracellular Na^+. (*A*) Typical original data show the currents in response to a double solution-exchange protocol, first from NMGCl to NaCl, and second from NaCl to NaCl + 10 mM alanine, as indicated by the bars (*top*). The pipette contained 140 mM SCN^-. (*B*) Current-voltage relationships of the alanine-sensitive anion current in the absence of Na^+ determined by subtraction from currents obtained at time points A-B, as indicated by the arrows in (*A*).

the intracellular anion composition constant. Because it carries larger anion current than $SNAT2_{WT}$, these anion substitution experiments were performed for $SNAT2_{H\text{-}304A}$. We chose an intracellular anion composition of 10 mM SCN^- and 130 mM Mes^- because it ensured that the reversal potentials were in the measurable range (−90 to + 60 mV) for the anions studied. Typical original data for SCN^- as the extracellular anion are shown in Fig. 9 *A*. The alanine-sensitive current was inwardly directed at potentials more positive than −60 mV, due to SCN^- inflow. The reversal potential was determined from average current voltage relationships, shown in Fig. 9 *B* as -50 ± 11 mV ($n = 3$). Similar experiments for other anions (Mes^-, Cl^-, Br^-, I^-, and NO_3^-) are shown in Fig. 9 *B* and representative original data for some of these anions are shown in Supplementary Materials Fig. 4. The SNAT2-specific currents were at least fivefold larger than the background in nontransfected cells. Table 1 lists the reversal potentials of the currents measured for these various anions. The reversal potential was more positive for these anions compared to SCN^-, suggesting that the permeability of $SNAT2_{H\text{-}304A}$ to SCN^- was the largest of the anions tested. The reversal potentials for other anions were between +14 mV to −11 mV. This determination of reversal potentials led to a general anion selectivity sequence of $SCN^- \gg NO_3^- > I^- > Br^- > Cl^- > Mes^-$, showing that the $SNAT2_{H\text{-}304A}$ anion conductance is selective for weakly hydrated, hydrophobic anions. Permeability ratios relative to SCN^- as calculated with the Goldman-Hodgkin-Katz voltage equation (29) are also listed in Table 1.

Anion flux mediated by NO_3^-, but not by SCN^-, is saturable

To further test the differences in permeation properties between nitrate and SCN^-, we determined the anion concentration dependence of leak currents mediated by $SNAT2_{H\text{-}304A}$. In the presence of 140 mM Na^+ in the extracellular solution inhibition of the leak anion current by 10 mM alanine was dependent on extracellular [SCN^-], as shown in Fig. 10 *A*. This concentration dependence was linear up to 126 mM SCN^- (Fig. 10 *B*), suggesting that a [SCN^-] as high as 126 mM was still far from being a saturating concentration. In contrast, alanine-sensitive current in the presence of different extracellular NO_3^- concentrations showed nonlinear behavior and saturated at high [NO_3^-] (Fig. 10 *C*). Kinetic analysis with a Michaelis-Menten-type relationship indicated that the K_m of $SNAT2_{H\text{-}304A}$ for NO_3^- was 29 ± 8 mM. These data suggest that NO_3^- transition through the anion-conducting pathway becomes rate limited at high NO_3^- concentrations by a concentration-independent process, one possibility being the anion dissociation process to the *trans*-side of the membrane (32). Thus, NO_3^- may spend more time associated with its ''binding site'' than SCN^-, which can explain why the current evoked by SCN^- is larger than the current evoked by NO_3^-.

DISCUSSION

SNAT2 is known to be alanine preferring and capable of transporting *N*-methylated and small aliphatic amino acids,

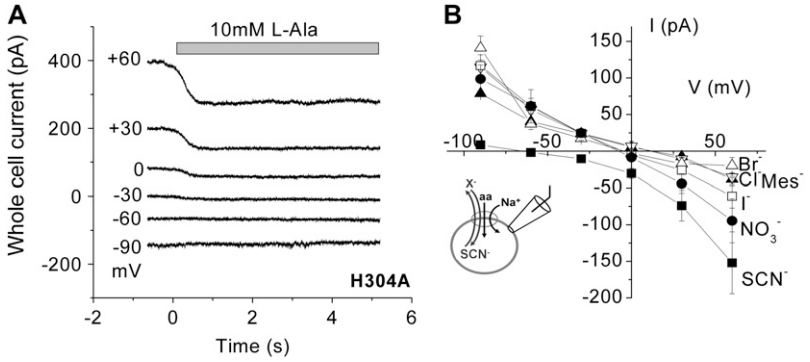

FIGURE 9 Anion selectivity of the transporter-associated anion conductance in $SNAT2_{H\text{-}304A}$-expressing cells. (*A*) Responses after a solution exchange from 0 mM alanine to 10 mM alanine (indicated by the *bar*) at membrane potentials ranging from −90 to +60 mV. The pipette solution contained 10 mM KSCN and 130 mM KMes, the bath solution contained 126 mM NaSCN. (*B*) Voltage dependence of alanine-sensitive currents in an external solution containing 126 mM Mes^- (▲), Cl^- (▽), Br^- (△), I^- (□), NO_3^- (●), and SCN^- (■) in the presence of 126 mM external Na^+ with 10 mM KSCN plus 130 mM internal KMes; 10 mM L-alanine was applied.

TABLE 1 Anion selectivity of the L-alanine-inhibited $SNAT2_{H\text{-}304A}$ anion conductance

Ion	Reversal potential (mV)	P_{X-}/P_{SCN-}
Methanesulfonate$^-$	+14 ± 2	0.04
Cl^-	+10 ± 6	0.05
Br^-	+1 ± 7	0.08
I^-	−5 ± 2	0.10
NO_3^-	−11 ± 4	0.12
SCN^-	−50 ± 11	1.00

Reversal potentials were determined after subtraction of the leak current from the total current. Recording conditions included various external anions as 126 mM sodium salts in the presence of 2 mM $CaGlu_2$, 2 mM $MgMes_2$, 30 mM Tris/Mes, pH 8.0. The internal solution contained 10 mM KSCN, 130 mM KMes, 2 mM $MgMes_2$, and 30 mM HEPES, pH 7.3. A total of 10 mM L-alanine was applied to the $SNAT2_{H\text{-}304A}$-expressing cells. Permeabilities relative to P_{SCN-} were calculated according to the Goldman-Hodgkin-Katz voltage equation (44).

and its amino acid transport is driven by Na^+ cotransport (4). Our functional data on SNAT2 expressed in HEK293 cells agree well with previously published functional data obtained with the *Xenopus* oocyte expression system. We confirm that electrogenic alanine transport by SNAT2 is voltage dependent, is [Na^+] dependent, and saturates with an apparent K_m for alanine of ~200 μM. It also accepts MeAIB as a transported substrate. Nontransfected cells showed only little currents in response to the application of alanine, glutamine, and MeAIB. Together, these results suggest that HEK293 cells are an adequate expression system for functional studies on SNAT2.

The main new finding of this study is that SNAT2 catalyzes a leak anion conductance that is inhibited by binding of transported substrates to the transporter. This inhibition is evidenced by the reduction of a tonic inward current by transported substrates in the presence of intracellular permeating anions, although the electrogenic transport current should be always inwardly directed under the forward transport conditions used. We interpret the results such that the apparent substrate-sensitive current is a sum of two current components: the substrate-induced electrogenic transport current and the substrate-inhibited anion current (Fig. 3, *E* and *F*). If permeating anions are present on the intracellular side, these substrate-sensitive current components have opposite direction. Therefore, the current reverses direction at a reversal potential that depends on the nature (Fig. 9) and concentration of the permeating anions (Fig. 5) and the transported substrate (Fig. 4). Although indirect activation of an anion conductance by SNAT2 through an accessory protein cannot be fully ruled out, we propose that the observed anion conductance is mediated directly by the SNAT2 protein.

The evidence for this interpretation is as follows: 1) Anion currents are inhibited by alanine with approximately the same apparent affinity (260 μM) as transport currents are activated (200 μM, Figs. 2 *C* and 3 *D*). This suggests that occupation of a single amino acid-binding site on SNAT2 by alanine is responsible for both of these effects. 2) Both current components increased with increasing expression levels of SNAT2 in the membrane (Supplementary Materials Fig. 1). If SNAT2 would activate an independent anion channel, it would be expected that the ratio between transport current and anion current, as well as the reversal potential, would vary with the expression levels of the protein. Our data on the anion conductance of SNAT2 can be explained by a kinetic model shown in Fig. 11, summarizing results presented in this work and previous results on the mechanism of SLC38 transporters (4). In this model Na^+ and amino acid, aa, bind sequentially to the empty transporter, T, to form the fully loaded transporter form, which can translocate the amino acid and Na^+ across the membrane. Substrate dissociation to the cytoplasm and relocation of the empty transporter have not been studied here but are shown to complete the model. Our data demonstrating that Na^+ activates anion current in the absence of amino acid suggest that Na^+ binds to the amino acid-free form of SNAT2, supporting the hypothesis of a Na^+ first, amino acid last binding sequence. The model assigns the largest anion conductance to the Na^+ bound, amino acid-free state, but the Na^+-free and amino acid-bound states are also anion conducting, although to a lesser extent (illustrated by the thickness of the *curved arrows* indicating the anion movement across the membrane associated with these specific states in Fig. 11).

Transport of alanine is independent of the presence of a permeating anion, since transport was still present with Mes^- as the only anion present on either side of the membrane. On

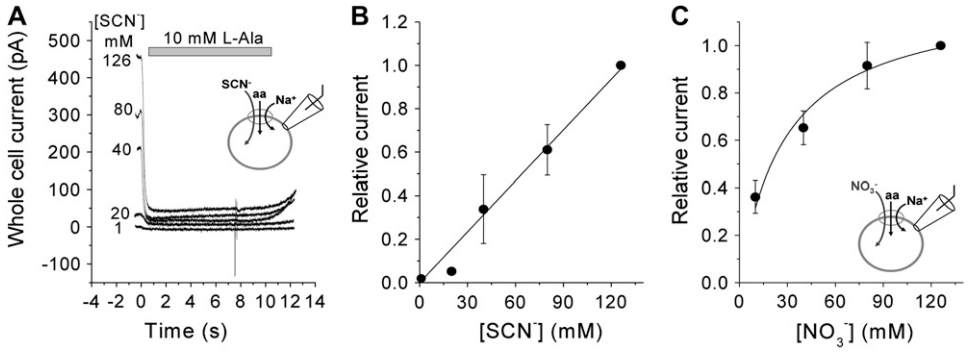

FIGURE 10 Anion currents carried by NO_3^- are saturable. (*A*) Typical currents induced by alanine (10 mM) at various external [SCN^-] concentrations at a holding potential of 0 mV. (*B*) and (*C*) show the determination of apparent K_m values for SCN^- (*B*) and NO_3^- (*C*) of anion binding to $SNAT2_{H\text{-}304A}$ by measuring the alanine-sensitive anion current at different extracellular [anion$^-$] (126 mM Na^+). The solid lines represent fits to the Hill equation with a Hill coefficient of $n = 1$. For SCN^- no K_m can be obtained because the current does not saturate within the concentration range tested. For NO_3^-, the K_m is 29 ± 8 mM.

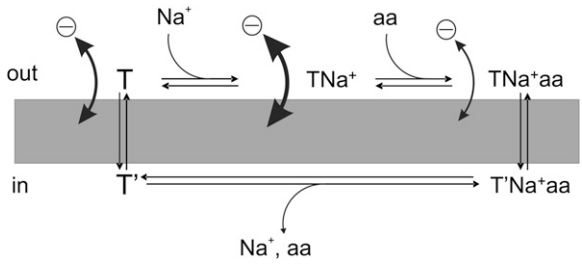

FIGURE 11 Assignment of the anion conductance to specific states in the kinetic model of amino acid-Na^+ cotransport by SNAT2. T and T′ are the transporters with the amino acid (*aa*) and Na^+-binding sites exposed to the extracellular side and the cytoplasm, respectively. The anion-conducting states are indicated by the curved arrows with thicker arrows indicating higher anion conductance.

the other hand, inhibition of the anion conductance is most likely also independent of alanine transport. This hypothesis is supported by the experiments with the H-304A mutant transporter catalyzing anion flux while alanine transport was impaired. These results suggest that the anion conductance is thermodynamically uncoupled from substrate and Na^+ transport. Similar observations have been made for the anion conductance of glutamate transporters, which is thermodynamically uncoupled from glutamate transport (22).

The SNAT2 leak anion conductance characterized here is stimulated in the presence of extracellular Na^+. However, some anion current is present in the absence of sodium ions, as demonstrated in the transporter with the mutation H-304A. In the mutant transporter, the combined application of Na^+ and alanine induces apparent outward current (with SCN^- in the recording pipette), due to the inhibition of the inwardly directed leak anion current in the absence of Na^+. Our data also suggest that the substrate-bound transporter is somewhat anion conducting because glutamine is less potent in inhibiting leak anion current than MeAIB and alanine (Fig. 4). Therefore, at least the glutamine-bound transporter must be anion conducting. Taken together, our data suggest that the anion conductance is modulated as the transporter moves through different states in the transport cycle (Fig. 11). These properties of the SNAT2 leak anion conductance are similar to the leak anion conductance of glutamate transporters (24). Both are stimulated in the presence of Na^+ and are inhibited by the binding of substrates or inhibitors. However, in contrast to SNAT2, glutamate transporters have an additional anion conductance that is gated by substrate binding (33–36). Because the SNAT2 anion conductance depends on the bound substrate, it can be speculated that substrates other than the ones tested here may activate the SNAT2 anion conductance instead of inhibiting it.

The anion selectivity sequence of the $SNAT2_{H\text{-}304}$ anion conductance was determined by anion substitution experiments. The conductance sequence was $SCN^- \gg NO_3^- > I^- > Br^- > Cl^- > Mes^-$. This conductance sequence is similar to those found for anion movement through glutamate transporters (SLC1) (22,37) and dicarboxylate transporters (SLC13 family) (38), showing a preference for hydrophobic anions, such as SCN^-. In some chloride channels, such as γ-aminobutyric acid receptors and Ca(Cl) channels, hydrophobic ions carry less current than Cl^-, although they are more permeant than chloride, as determined through reversal potential measurements (39,40). This behavior is explained by the tighter binding of hydrophobic anions to their binding site(s) in the channel, leading to rate limitation by anion unbinding to the *trans*-side and, thus, lower channel conductance. The SNAT2 anion conductance differs from these anion channels in that the less hydrophobic anion nitrate shows saturation kinetics, whereas the more hydrophobic SCN^- does not, indicating that NO_3^- binds with a higher apparent affinity to its site in the pore. A similar observation was made for the ions nitrate and chloride in the glutamate transporter anion conductance, with Cl^- carrying less current but binding with a higher affinity. Thus, it appears that SCN^- carries the larger current through SNAT2 because its rate of movement through the pore is not limited by slow anion unbinding. As in glutamate transporters and in contrast to classical anion channels, the SNAT2 anion conductance has a small unitary conductance. We have attempted noise analysis of Na^+-activated or alanine-inhibited anion currents but were unable to observe any difference in noise in the absence or presence of activator/inhibitor (the variance σ^2 of the current recordings in the presence of Na^+ was ≤ 0.05 pA^2 at mean current amplitudes ranging from 20 to 100 pA, 0 mV). We conclude that the unitary current carried by the transporter with SCN^- as the anion is <1 fA at 0 mV transmembrane potential. Such low unitary current values are typical for Na^+-driven transporter-associated anion conductances (26,37,41) but untypical for classical anion channels.

Other anion channels exhibit multiply occupied pores, resulting in anomalous concentration dependencies of biionic reversal potentials (42). We have determined reversal potentials under biionic conditions (using SCN^- and nitrate as the permeant anions), as described in Melzer et al. (26) and Dani (43), and found that the reversal potential was dependent on the extracellular [NO_3^-] (Supplementary Materials Fig. 3). Although this finding may indicate a multiply occupied pore, other explanations are also possible for this behavior, such as modulation of anion selectivity by a *trans*-anion (44). However, these complex properties of the SNAT2-associated anion conductance duplicate the ones found in glutamate transporters (26), indicating that the mechanistic principles of anion permeation may be similar in these two protein families, although they are structurally not related.

SNAT2 with the mutation H-304A is defective in alanine transport at voltages ≤ 0 mV. At positive voltages a small alanine-induced current was observed. These results may suggest that the H-304A mutation changes the voltage dependence of alanine transport. Whereas transport by $SNAT2_{WT}$ is accelerated by negative transmembrane potentials, as expected for a process in which positive charge is moved into the cell, transport by $SNAT2_{H\text{-}304A}$ is inhibited by negative

voltages. It can be speculated that an individual reaction step in the transport cycle with opposite voltage dependence becomes rate limiting in the $SNAT2_{H\text{-}304A}$ protein that is masked in the wild-type transporter. To test exactly which step(s) are affected by the mutation will require further experimentation. Alternatively, $SNAT2_{H\text{-}304A}$ may catalyze a cation leak conductance, allowing K^+ to leave the cell at positive potentials. Our data presented here do not allow us to differentiate between these two possibilities. In any case, the H-304A mutation resulted in large anion leak currents (up to 400 pA), indicating that it is possible to abolish substrate transport without inhibiting the leak anion conductance. A similar behavior has been reported for the glutamate transporter subtype EAAT1 (36), in which modification of the V-449C residue with sulfhydryl reagents abolished glutamate transport but not the glutamate-gated anion conductance. This finding was interpreted such that anions and transported substrate have separate translocation pathways in the protein. This might also be possible for SNAT2 anion and substrate movement across the membrane. If this is the case, it might be possible to generate mutant transporters that still catalyze transport but no anion conductance.

Anion conductances associated with other secondary transporters appear to be of physiological importance. For example, it has been shown that activation of a chloride conductance in the dopamine transporter alters neuronal excitability (45). Here, we show that substrate-induced SNAT2 currents do not reverse within the voltage range of -90 to $+60$ mV with Cl^- as the main extracellular anion. This finding suggests that the transport current dominates the total SNAT2 current at physiological conditions. Since the Cl^- conductance is $\sim$7% of the SCN^- conductance, we can estimate that at $+60$ mV $\sim$20 pA of current is carried by SNAT2 leak chloride conductance in the SNAT2-transfected HEK293 cells, which is $\sim$15% of the transport current. Although this value would depend on the expression level of SNAT2 in each respective cell, it is reasonable to assume that the SNAT2 chloride conductance adds to other background anion conductances to keep the resting membrane at hyperpolarized levels suited for rapid amino acid transport. In the brain, SNAT1 and 2 are expressed in neurons (46). It was shown that glia cells influence neuronal activity by modulating glutamine-driven Na^+ influx into neurons and by controlling glutamate availability to neurons through glutamine transport (46). The anion conductance could be a third mechanism by which glia cells could influence neuronal activity through SNAT2. In the presence of high extracellular amino acid concentrations the SNAT2 anion conductance is inhibited, leading to increased excitability of neurons.

In summary, this study represents the first report of the existence of an anion leak pathway mediated by a Na^+-coupled neutral amino acid transporter belonging to the SLC38 protein family. This anion leak conductance is inhibited differentially by transported amino acid substrates and is potentiated by the presence of extracellular Na^+, but smaller anion currents are also present in the total absence of sodium ions. The leak anion conductance is specific for hydrophobic anions. The amino acid residue H-304 probably plays an important role in regulating the relative magnitudes of the anion current component and the transport current. Our new data on this SLC38 family transporter add to the mounting evidence that the existence of anion-conducting pathways are a general property of Na^+-coupled secondary transporters.

SUPPLEMENTARY MATERIAL

An online supplement to this article can be found by visiting BJ Online at http://www.biophysj.org.

We thank Dr. H. Varoqui for providing the SNAT2 cDNA and Dr. T. Rauen for the pBK-CMVΔ expression plasmid.

This work was supported by a grant from the Florida Department of Health (04NIR-07) awarded to C.G.

REFERENCES

1. Johnson, L. W., and C. H. Smith. 1988. Neutral amino acid transport systems of microvillous membrane of human placenta. *Am. J. Physiol.* 254:C773–C780.
2. Sugawara, M., T. Nakanishi, Y. J. Fei, W. Huang, M. E. Ganapathy, F. H. Leibach, and V. Ganapathy. 2000. Cloning of an amino acid transporter with functional characteristics and tissue expression pattern identical to that of system A. *J. Biol. Chem.* 275:16473–16477.
3. Bode, B. P. 2001. Recent molecular advances in mammalian glutamine transport. *J. Nutr.* 131:2475S–2485S.
4. Yao, D., B. Mackenzie, H. Ming, H. Varoqui, H. Zhu, M. A. Hediger, and J. D. Erickson. 2000. A novel system A isoform mediating Na+/neutral amino acid cotransport. *J. Biol. Chem.* 275:22790–22797.
5. Shotwell, M. A., D. W. Jayme, M. S. Kilberg, and D. L. Oxender. 1981. Neutral amino acid transport systems in Chinese hamster ovary cells. *J. Biol. Chem.* 256:5422–5427.
6. Christensen, H. N., D. L. Oxender, M. Liang, and K. A. Vatz. 1965. The use of N-methylation to direct route of mediated transport of amino acids. *J. Biol. Chem.* 240:3609–3616.
7. Oxender, D. L., and H. N. Christensen. 1963. Distinct mediating systems for the transport of neutral amino acids by the Ehrlich cell. *J. Biol. Chem.* 238:3686–3699.
8. Palii, S. S., H. Chen, and M. S. Kilberg. 2004. Transcriptional control of the human sodium-coupled neutral amino acid transporter system A gene by amino acid availability is mediated by an intronic element. *J. Biol. Chem.* 279:3463–3471.
9. Kilberg, M. S., and O. W. Neuhaus. 1977. Hormonal regulation of hepatic amino acid transport. *J. Supramol. Struct.* 6:191–204.
10. Mackenzie, B., and J. D. Erickson. 2004. Sodium-coupled neutral amino acid (system N/A) transporters of the SLC38 gene family. *Pflueg. Arch.* 447:784–795.
11. Hatanaka, T., W. Huang, H. Wang, M. Sugawara, P. D. Prasad, F. H. Leibach, and V. Ganapathy. 2000. Primary structure, functional characteristics and tissue expression pattern of human ATA2, a subtype of amino acid transport system A. *Biochim. Biophys. Acta.* 1467:1–6.
12. Varoqui, H., H. Zhu, D. Yao, H. Ming, and J. D. Erickson. 2000. Cloning and functional identification of a neuronal glutamine transporter. *J. Biol. Chem.* 275:4049–4054.
13. Mackenzie, B., M. K. Schafer, J. D. Erickson, M. A. Hediger, E. Weihe, and H. Varoqui. 2003. Functional properties and cellular distribution of the system A glutamine transporter SNAT1 support specialized roles in central neurons. *J. Biol. Chem.* 278:23720–23730.

14. McGivan, J. D., and M. Pastor-Anglada. 1994. Regulatory and molecular aspects of mammalian amino acid transport. *Biochem. J.* 299:321–334.

15. Chaudhry, F. A., D. Schmitz, R. J. Reimer, P. Larsson, A. T. Gray, R. Nicoll, M. Kavanaugh, and R. H. Edwards. 2002. Glutamine uptake by neurons: interaction of protons with system A transporters. *J. Neurosci.* 22:62–72.

16. Albers, A., A. Broer, C. A. Wagner, I. Setiawan, P. A. Lang, E. U. Kranz, F. Lang, and S. Broer. 2001. Na+ transport by the neural glutamine transporter ATA1. *Pflueg. Arch.* 443:92–101.

17. Hirayama, B. A., M. P. Lostao, M. Panayotova-Heiermann, D. D. Loo, E. Turk, and E. M. Wright. 1996. Kinetic and specificity differences between rat, human, and rabbit Na+-glucose cotransporters (SGLT-1). *Am. J. Physiol.* 270:G919–G926.

18. Pajor, A. M., and E. M. Wright. 1992. Cloning and functional expression of a mammalian Na+/nucleoside cotransporter. A member of the SGLT family. *J. Biol. Chem.* 267:3557–3560.

19. Murer, H., I. Forster, and J. Biber. 2004. The sodium phosphate cotransporter family SLC34. *Pflueg. Arch.* 447:763–767.

20. Fairman, W. A., R. J. Vandenberg, J. L. Arriza, M. P. Kavanaugh, and S. G. Amara. 1995. An excitatory amino-acid transporter with properties of a ligand-gated chloride channel. *Nature.* 375:599–603.

21. Picaud, S. A., H. P. Larsson, G. B. Grant, H. Lecar, and F. S. Werblin. 1995. Glutamate-gated chloride channel with glutamate-transporter-like properties in cone photoreceptors of the tiger salamander. *J. Neurophysiol.* 74:1760–1771.

22. Wadiche, J. I., S. G. Amara, and M. P. Kavanaugh. 1995. Ion fluxes associated with excitatory amino acid transport. *Neuron.* 15:721–728.

23. Grewer, C., N. Watzke, M. Wiessner, and T. Rauen. 2000. Glutamate translocation of the neuronal glutamate transporter EAAC1 occurs within milliseconds. *Proc. Natl. Acad. Sci. USA.* 97:9706–9711.

24. Otis, T. S., and C. E. Jahr. 1998. Anion currents and predicted glutamate flux through a neuronal glutamate transporter. *J. Neurosci.* 18: 7099–7110.

25. Billups, B., D. Rossi, and D. Attwell. 1996. Anion conductance behavior of the glutamate uptake carrier in salamander retinal glial cells. *J. Neurosci.* 16:6722–6731.

26. Melzer, N., A. Biela, and C. Fahlke. 2003. Glutamate modifies ion conduction and voltage-dependent gating of excitatory amino acid transporter-associated anion channels. *J. Biol. Chem.* 278:50112–50119.

27. Arriza, J. L., S. Eliasof, M. P. Kavanaugh, and S. G. Amara. 1997. Excitatory amino acid transporter 5, a retinal glutamate transporter coupled to a chloride conductance. *Proc. Natl. Acad. Sci. USA.* 94:4155–4160.

28. Meinild, A. K., H. H. Sitte, and U. Gether. 2004. Zinc potentiates an uncoupled anion conductance associated with the dopamine transporter. *J. Biol. Chem.* 279:49671–49679.

29. Goldman, D. E. 1943. Potential, impedance, and rectification in membranes. *J. Gen. Physiol.* 27:37–60.

30. Reimer, R. J., F. A. Chaudhry, A. T. Gray, and R. H. Edwards. 2000. Amino acid transport system A resembles system N in sequence but differs in mechanism. *Proc. Natl. Acad. Sci. USA.* 97:7715–7720.

31. Tao, Z., Z. Zhang, and C. Grewer. 2006. Neutralization of the aspartic acid residue Asp-367, but not Asp-454, inhibits binding of Na+ to the glutamate-free form and cycling of the glutamate transporter EAAC1. *J. Biol. Chem.* 281:10263–10272.

32. Dani, J. A., J. A. Sanchez, and B. Hille. 1983. Lyotropic anions. Na channel gating and Ca electrode response. *J. Gen. Physiol.* 81:255–281.

33. Borre, L., M. P. Kavanaugh, and B. I. Kanner. 2002. Dynamic equilibrium between coupled and uncoupled modes of a neuronal glutamate transporter. *J. Biol. Chem.* 277:13501–13507.

34. Ryan, R. M., and R. J. Vandenberg. 2002. Distinct conformational states mediate the transport and anion channel properties of the glutamate transporter EAAT-1. *J. Biol. Chem.* 277:13494–13500.

35. Shachnai, L., K. Shimamoto, and B. I. Kanner. 2005. Sulfhydryl modification of cysteine mutants of a neuronal glutamate transporter reveals an inverse relationship between sodium dependent conformational changes and the glutamate-gated anion conductance. *Neuropharmacology.* 49:862–871.

36. Seal, R. P., Y. Shigeri, S. Eliasof, B. H. Leighton, and S. G. Amara. 2001. Sulfhydryl modification of V449C in the glutamate transporter EAAT1 abolishes substrate transport but not the substrate-gated anion conductance. *Proc. Natl. Acad. Sci. USA.* 98:15324–15329.

37. Wadiche, J. I., and M. P. Kavanaugh. 1998. Macroscopic and microscopic properties of a cloned glutamate transporter/chloride channel. *J. Neurosci.* 18:7650–7661.

38. Oshiro, N., and A. M. Pajor. 2005. Functional characterization of high-affinity Na(+)/dicarboxylate cotransporter found in Xenopus laevis kidney and heart. *Am. J. Physiol. Cell Physiol.* 289:C1159–C1168.

39. Bormann, J., O. P. Hamill, and B. Sakmann. 1987. Mechanism of anion permeation through channels gated by glycine and gamma-aminobutyric acid in mouse cultured spinal neurones. *J. Physiol.* 385:243–286.

40. Hartzell, C., I. Putzier, and J. Arreola. 2005. Calcium-activated chloride channels. *Annu. Rev. Physiol.* 67:719–758.

41. Palmer, M. J., H. Taschenberger, C. Hull, L. Tremere, and H. von Gersdorff. 2003. Synaptic activation of presynaptic glutamate transporter currents in nerve terminals. *J. Neurosci.* 23:4831–4841.

42. Hebeisen, S., H. Heidtmann, D. Cosmelli, C. Gonzalez, B. Poser, R. Latorre, O. Alvarez, and C. Fahlke. 2003. Anion permeation in human ClC-4 channels. *Biophys. J.* 84:2306–2318.

43. Dani, J. A. 1989. Open channel structure and ion binding sites of the nicotinic acetylcholine receptor channel. *J. Neurosci.* 9:884–892.

44. Hille, B. 2001. Ion Channels of Excitable Membranes. Sinauer Associates, Sunderland, MA.

45. Ingram, S. L., B. M. Prasad, and S. G. Amara. 2002. Dopamine transporter-mediated conductances increase excitability of midbrain dopamine neurons. *Nat. Neurosci.* 5:971–978.

46. Armano, S., S. Coco, A. Bacci, E. Pravettoni, U. Schenk, C. Verderio, H. Varoqui, J. D. Erickson, and M. Matteoli. 2002. Localization and functional relevance of system A neutral amino acid transporters in cultured hippocampal neurons. *J. Biol. Chem.* 277:10467–10473.